JMEPEG (1996) 5:691-694

Transmission Electron Microscopy Study of Stress-Ruptured Aged 304H Stainless Steel after Prolonged Exposure in Service

A. Sengupta and M. Balogh

Type 304H stainless steel is widely used for long-term, high-temperature applications, e.g., superheater tubes in steam generators. The 304H stainless steel tube in the present investigation has been exposed in service to a temperature range of 565 to 595 °C for a prolonged period (in excess of 20 years).

Metallographic and transmission electron microscopic analysis was carried out on exposed material to study the nature and type of precipitates formed in this material after prolonged exposure in service.

Keywords

exposure, stainless steel, stress rupture, TEM

1. Introduction

AGED 304H stainless steel is widely used for critical high-temperature applications in the utility industries, e.g., superheater tubes in steam generators where it can undergo extensive creep. Prolonged exposure in service at high temperature can cause precipitation of carbides (Ref 1-4), resulting in degradation of metallurgical microstructures. This can influence the creep behavior, i.e., cavity growth (Ref 5, 6), steady-state creep rate, rupture time, and stress-rupture properties of the material (Ref 7-9). Investigation of the degradation of aged 304H stainless steel after long-term exposure in service will be helpful in predicting the remaining life of such structural components.

The aim of the present study was to examine and evaluate changes in the metallurgical microstructure of aged 304H stainless steel after prolonged exposure in service. Detailed transmission electron microscopy (TEM) was carried out on exposed material to determine the nature and the type of the precipitates formed after long-term service exposure.

2. Material and Experimental Procedure

The unexposed material was an ASTM grade A213 (Ref 10) austenitic stainless steel. The chemical composition of the material studied is shown in Table 1. The material was taken from a superheater tube which had been exposed to an elevated temperature of 593 °C for over twenty years. The metallographic techniques employed in this study consisted of microstructural examination by Phillips EM430 TEM operated at 300 KeV. Specimens were cut by a diamond wafer blade to approximately 0.5 mm thickness. These specimens were mechanically polished to a thickness of approximately 300 μm. A 3 mm disc was then punched and mechanically thinned down to 100 μm for electropolishing. For electropolishing, a Fishione twinjet electropolisher was used with a voltage of 35 V at a temperature of 0 °C. The electropolishing solution was a mixture of 6% perchloric acid, 35% butylcellusolve, and 59% methanol. At least two specimens were examined to characterize the precipitate types.

A Sengupta, Department of Materials Science and Engineering, Wayne State University, 5050 Anthony Wayne Drive, Detroit, MI 48202, USA, presently with GM-Ovonic, Troy, MI 48084; and **M. Balogh,** Analytical Chemistry Department, General Motors Technical Center, 30500 Mound Road 1-6, Box 9055, Warren, MI 48090-9055, USA.

3. Results and Discussion

TEM analysis of the exposed material showed both intragranular and grain boundary (GB) precipitates. The intragranular precipitates are shown in Fig. 1. The intragranular precipitates are cube-shape and of the order of 100 nm across. The precipitates were identified by electron diffraction to be $M_{23}C_6$ type. The electron diffraction pattern from the area shown in Fig. 1 is shown in Fig. 2. The precipitates have a cube-on-edge orientation with the austenite matrix of:

$$(111)_{M23C6} \parallel (111)_\gamma$$

$$[110]_{M23C6} \parallel [110]_\gamma$$

The cube-on-cube orientation has been observed by others (Ref 11). Elemental x-ray maps shown in Fig. 3 confirm the presence of chromium-rich $M_{23}C_6$-type precipitates. EDX spot analysis shows higher concentration of chromium in the precipitate, as shown in Table 2.

Table 1 Chemical composition of the material

Element	wt%
C	0.05
Mn	0.5
S	0.0003
Cr	18.3
Mo	0.2
Si	0.62
P	0.023
Ni	8.5
Cu	0.14
Fe	bal

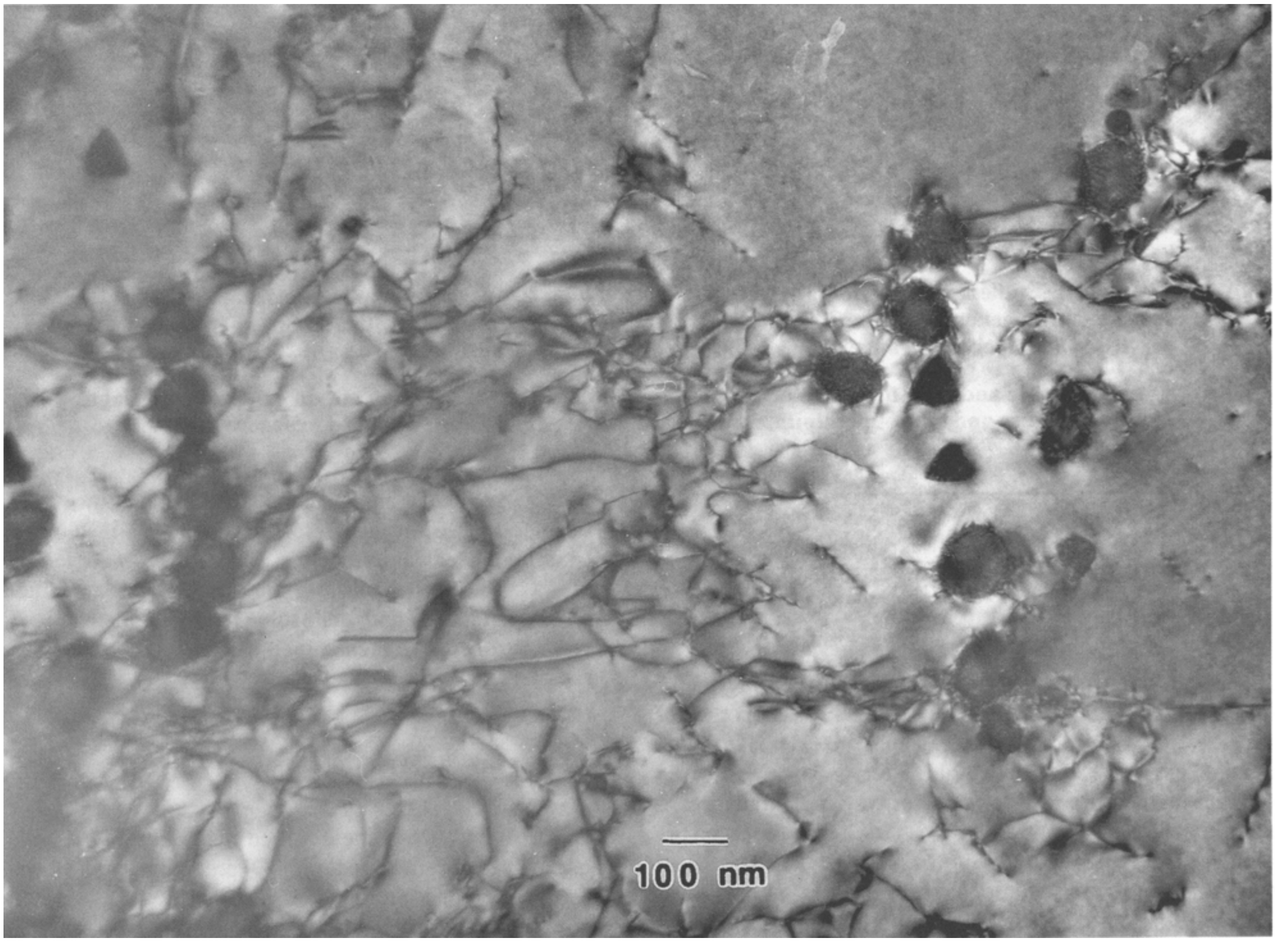

Fig. 1 TEM micrograph of precipitates. 80,000×

Fig. 2 Selected area diffraction pattern of the precipitate. Zone axis is <111>.

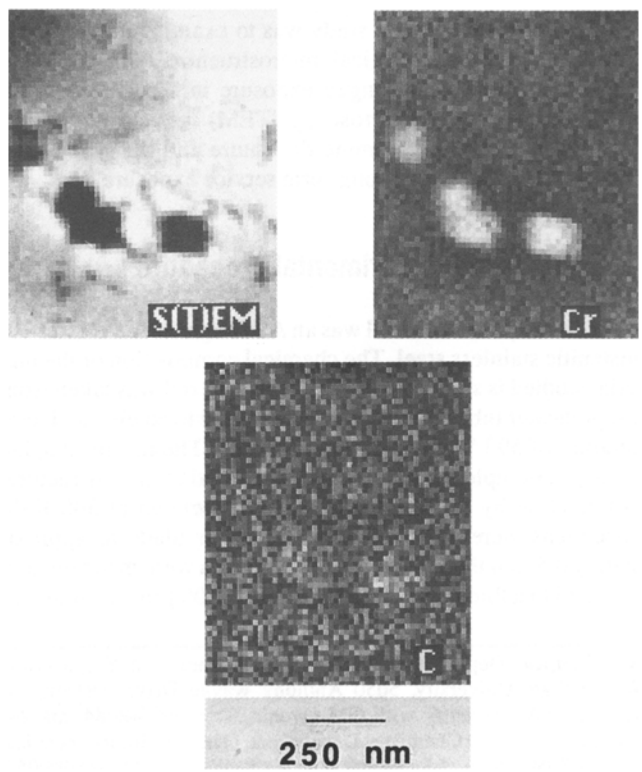

Fig. 3 Digital X-ray mapping of precipitate. 40,000×

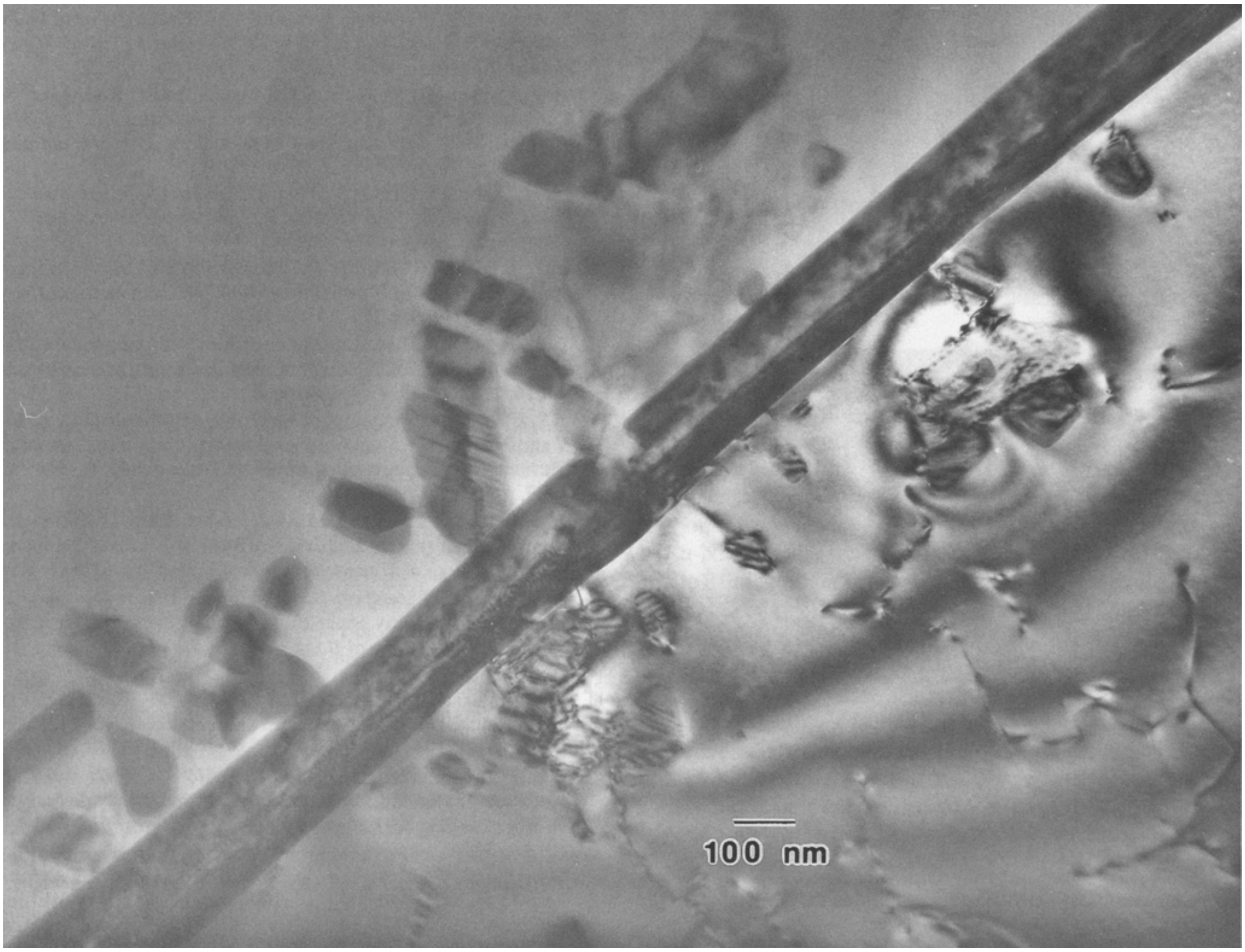

Fig. 4 TEM micrograph at the grain boundary. 80,000×

Table 2 Energy dispersive spectroscopy analysis

Site	%Ni	%Fe	%Cr	%Si	%P	%Mo
Precipitate, matrix	6	48	42	0.4	0.1	1.2
Precipitate, near GB	4	33	59	0.4	<0.1	1.7
GB	5	64	28	0.4	<0.1	0.8
Matrix	9	73	15	0.5	0.2	0.2
Matrix, near GB	9	77	13	0.3	<0.1	0.1

TEM micrograph in Fig. 1 shows interaction between precipitate and dislocations. The dislocations act as the preferential sites for nucleation of $M_{23}C_6$ precipitates within grains. The driving force for this massive precipitation appears to be carbon supersaturation (Ref 12), enhanced diffusion of the chromium and carbon rejected by the austenitic matrix (Ref 13). The diffusion of chromium and carbon is further enhanced by nonequilibrium vacancies generated during exposure to high temperature.

The GB precipitates are shown in the TEM micrograph in Fig. 4. The precipitates appear to be large plate type approximately 100 nm thick. Electron diffraction data show that the GB precipitates are of the $M_{23}C_6$ type. Precipitates adjacent to the GB show Moire fringe, indicating coherent precipitates (Ref 14). Elemental x-ray maps collected at the GB are shown in Fig. 5. The GB has a higher chromium concentration, as shown in Table 2. The iron concentration is higher at the interface of matrix and GB precipitates and low within the GB.

4. Conclusions

- Long-term exposure of 304H stainless steel at elevated temperatures produced both intragranular and grain boundary precipitates.
- Both intragranular and grain boundary precipitates were found to be of $M_{23}C_6$ type.
- Precipitates were found to be chromium rich.
- Intragranular precipitates were found to be cubic in shape and have a cube-on-cube relation to the matrix.
- High iron concentrations were observed at the grain boundary precipitates and matrix interface.

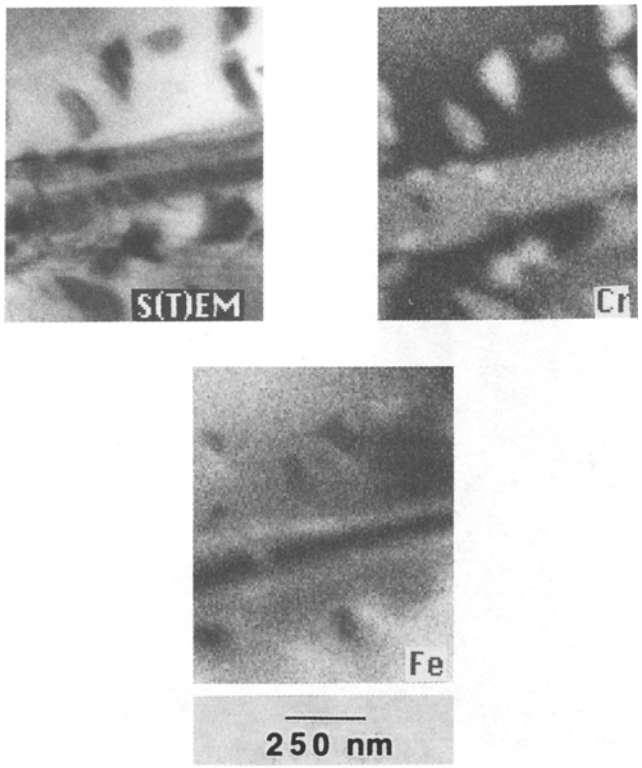

Fig. 5 Digital X-ray mapping of grain boundary. 40,000×

References

1. B. Weiss and R. Stickler, Phase Instabilities during High Temperature Exposure of 316 Austenitic Steel, *Metallurgical Transactions A,* Vol 3, 1972, p 851
2. A.A. Tavasoli, A. Bisson, and R. Soulat, Ferrite Decomposition in Austenitic Stainless Steel Weld Metals, *Metal Science,* Vol 18, 1984, p 345
3. S. Ahila, S. Ramakrishna Iyer, and V.M. Radhakrishnan, High Temperature Stability of 2.25Cr-1Mo Steel during Creep, *Materials at Higher Temperatures,* Vol 12, 1994, p 5
4. M.D. Mathew, G. Sasikala, S.L. Mannan, and P. Rodriguez, A Comparative Study of Creep Rupture Properties of Type 316 Stainless Steel Base and Weld Metals, *J Engg. Materials and Technology,* Vol 115, 1993, p 163
5. R.A. Varin and J. Haftek, Structural Changes in a Ferrite Heat-resistant Steel After Long-term Service, *Materials Science and Engineering,* Vol 62, 1984, p 129
6. R.G. Baker and J. Nutting, The Tempering of 2.25Cr-1Mo Steel after Quenching and Normalizing, *Iron and Steel Institute Journal,* Vol 192, 1959, p 257
7. T. Wada and V.A. Biss, Restoration of Elevated Temperature Tensile Strength in 2.25Cr-1Mo Steel, *Metallurgical Transactions A,* Vol 16, 1983, p 845
8. N.S. Cheruvu, Degradation of Mechanical Properties of Cr-Mo-V and 2.25Cr-1Mo Steel Components after Long-term Service at Elevated Temperature, *Metallurgical Transactions A,* Vol 20, 1989, p 87
9. W.B. Jones and J.A. Van Den Avyle, Substructure and Strengthening Mechanisms in 2.25Cr-1Mo Steel at Elevated Temperature, *Metallurgical Transactions A,* Vol 11, 1980, p 1275
10. ASTM A 213, "Standard Specification for Seamless Ferritic and Austenitic Alloy Steel Boiler, Superheater and Heat Exchanger Tubes," *Annual Book of ASTM Standards,* Vol 0.1.01, 1994, p 109
11. L.K. Singhal and J.W. Martin, The Growth of $M_{23}C_6$ Carbides on Grain Boundaries in an Austenitic Stainless Steel, Vol 242, May 1986, p 814-819
12. K.B.S. Rao, H. Schuster, and G.R. Halford, On Massive Carbide Precipitation during High Temperature Low Cycle Fatigue in Alloy 800H, *Scripta Metallurgica et Materialia,* Vol 31, 1994, p 381
13. M. Ahmad, K.A. Shoaib, M.A. Shaikh, and J.A. Akhtar, Identification of Surface Carbides and Spinels in Welded Austenitic Stainless Steels, *Journal of Materials Science,* Vol 29, 1994, p 1169
14. P.H. Pumphrey and I.W. Edington, The Structure of the Semicoherent Interface between Grain Boundary Nucleated M23C6 and Austenitic Stainless Steel, *Acta Metall.,* Vol 22, Jan 1974, p 89-94